

REGIOSELECTIVE ISOPROPYLATION OF DINUCLEAR AROMATICS OVER DEALUMINATED MORDENITE CATALYSTS

Andrew D. Schmitz and Chunshan Song

Department of Materials Science and Engineering
Fuel Science Program, 209 Academic Projects Building
Pennsylvania State University, University Park, PA 16802

Keywords: naphthalene, biphenyl, shape-selective alkylation

Summary

Selective addition of propylene to naphthalene or biphenyl over dealuminated H-mordenite (HM) catalysts is being used to produce 2,6-diisopropyl-naphthalene (2,6-DIPN) and 4,4'-diisopropylbiphenyl (4,4'-DIPB), respectively. When oxidized, these selectively substituted dinuclear aromatics become monomers for liquid crystalline polymers and engineering plastics.¹⁻⁵ We, and others, have shown that HM dealumination increases alkylation regioselectivity for isopropylation of binuclear aromatics.⁶⁻¹⁶ In this paper, we more closely examine the effects of HM dealumination on catalyst activity and regioselectivity, as well as effects on catalyst physical properties.

Two different mordenites were dealuminated by mineral acid leaching, HM14 and HM38, having $\text{SiO}_2/\text{Al}_2\text{O}_3$ (mol ratio) of 14 and 38, respectively. For naphthalene isopropylation, dealumination of HM14 increases the 2,6-DIPN isomer selectivity from 30 to 60%. Dealumination of HM38 gives similar results but with lower regioselectivity. For comparison, 4,4'-DIPB regioselectivity was examined in biphenyl isopropylation over a series of mordenites with $\text{SiO}_2/\text{Al}_2\text{O}_3$ 14-230. Selectivity for the 4,4'-isomer increased from 66 to 87%. Therefore, increased selectivity for the slimmest diisopropyl-isomer with dealumination is a general property: it occurs with different mordenite starting materials and different, but similar in size and shape, reactant molecules.

Selectivity for β -substitution of naphthalene seems to correlate with changes in HM mesopore volume brought about by dealumination. An increase in the mesopore volume is mirrored by an increase in 2,6-DIPN isomer selectivity. HM micropore volumes do not change appreciably. It has been shown that the two $\beta\beta$ -disubstituted naphthalenes have nearly identical critical diameters, but 2,6-DIPN has a somewhat more linear structure than 2,7-DIPN.^{3,6} Consequently, 2,6-DIPN has a lower activation energy for diffusion in HM.⁶ This explains why HM catalysts typically give 2,6/2,7 DIPN isomer ratios greater than unity. We have used X-ray powder diffraction to measure the decrease in HM unit cell volumes caused by dealumination. The 2,6/2,7 DIPN ratio shows an approximate inverse relationship with the unit cell volumes. A probable explanation is that the unit cell contractions caused by dealumination decrease the channel diameter, slightly, resulting in more snug fit for the $\beta\beta$ -disubstituted isomers in the channels. As a consequence, the difference in diffusion rates for 2,6- and 2,7-DIPN is magnified.

Experimental

Catalyst Preparation. The procedures used in this work have been described earlier.⁵ Mordenite catalysts CBV 10A (NaM14), CBV 20A (HM21) and CBV 30A (HM38) were supplied as 10 μm average particle size powders (PQ Corporation). HM14 was generated from NaM14 by sodium-exchanged with 1 M NH_4Cl . Dealumination was accomplished by stirring HM in aqueous hydrochloric or nitric acid at reflux temperature. Time and acid concentration were varied to control the extent of aluminum removal. All catalysts were calcined 5.5 h at 465 °C except HM230. HM230 was prepared according to a procedure described by Lee et al. for extensive aluminum removal.¹⁶ Accordingly, NaM14 was first treated at reflux with 1 M HCl to generate the HM54 sample. In the second step, HM54 was calcined at 700 °C and treated with 6 M HNO_3 , followed by final calcination at 700 °C. Samples were dissolved using lithium metaborate fusion and analyzed for silicon, aluminum and sodium by ICP-AES. Sorption data and residual sodium content for the catalysts are listed in Table 1.

Catalyst Evaluation. As described previously, catalyst testing was done in a tubing-bomb batch reactor charged with 0.10 g catalyst, 1.0 g (7.8 mmol) naphthalene, and 0.66 g (15.6 mmol) propylene.⁵ Naphthalene and biphenyl (Aldrich, 99% grades) and propylene (Matheson, 99.5% minimum, polymer purity) were used as supplied. Solution products were analyzed by GC-MS and GC-FID for qualitative and quantitative analyses, respectively, using a 30m x 0.25mm DB-17 (J&W Scientific) column.

X-ray powder diffraction (XRD) was done on a Scintag 3100 diffractometer using nickel-filtered $\text{Cu K}\alpha$ radiation. The $\text{Cu K}\alpha_2$ component was stripped from the patterns using the standard Scintag algorithm, so the wavelength used in the calculations is 1.540598 Å. Samples were mixed with ca. 10 wt% -325 mesh silicon internal standard for 2 θ corrections. The scan rate was 0.5° 2 θ /min with 0.02° steps. XRD pattern indexing and determination of lattice constants for HM (CMC2₁ space group) was done using the JCPDS-NBS*LSQ82 unit cell refinement computer program.¹⁷ This program minimizes the sum S defined in equation 1, where θ^{corr} are

$$S = \sum w_{hkl} (\theta_{hkl}^{\text{corr}} - \theta_{hkl}^{\text{calc}})^2 \quad (1)$$

the observed Bragg angles, corrected for instrumental and physical peak shifts, and θ^{calc} are calculated from the current unit cell parameters and the weighting factors w_{hkl} . Starting values for θ^{calc} are determined from the input unit cell parameters which are then adjusted, using a nonlinear least-squares method, to minimize S . This approach can lead to cell parameters accurate to a few parts in 10,000.¹⁷

Sorption analyses were done on either of two automated instruments: a Coulter SA 3100, or Quantachrome Autosorb. Samples were outgassed at 400 °C. Multipoint surface areas were calculated by the BET method. Micropore volumes were calculated using the T-plot method.

Results and Discussion

Isopropylation of Naphthalene. Catalyst test data for the two series of dealuminated HM catalysts is presented in Table 2. Greater than 98% of the products are isopropyl-naphthalenes (IPN's). The predominant side reactions result in small amounts of alkylnaphthalenes that are not solely isopropyl-substituted. Mass balances are greater than 96% in all cases, with material losses being primarily attributed to carbonaceous deposits on the catalyst.

The effects of dealumination on catalyst performance are shown in graphically in Figures 1-3. HM54 has abnormally low activity so its data for were omitted from these graphs because. HM230 has higher activity than expected, apparently due the higher activation temperature used in its preparation. Both HM14- and HM38 derived catalysts show similar activity patterns: naphthalene conversion first increases, then decreases as aluminum is removed from the lattice (volcano plots, Figure 1). This type of activity trend is quite common for HM and is due to the decreasing acid site density and increasing acid site strength that occurs with dealumination as discussed elsewhere.^{6,18-19} Both series of catalysts show a severe loss in activity at high $\text{SiO}_2/\text{Al}_2\text{O}_3$ ratios, probably due to gross depletion of acid sites. HM38-derived catalysts retain reasonable activity to higher ratios, indicative of higher acid site concentrations. HM93 (from HM38) shows a moisture loss on ignition 2.5 times the amount desorbed from HM90 (from HM14). This also suggests that HM38-derived catalysts have higher acid site concentrations than HM14-derived catalysts at the same $\text{SiO}_2/\text{Al}_2\text{O}_3$ ratio.

As shown in Figure 2, DIPN yield and selectivity are increased by dealumination up to the same maxima defined in Figure 1. Beyond these maxima, monoalkylation dominates and TriPN+ production falls to near zero. However, β -substitution selectivity (%2-MIPN and %2,6-DIPN) continues to increase with more extensive aluminum removal (Figure 3). This means that a larger fraction of the naphthalene and 2-MIPN molecules are reacting within the confines of the HM channels where α -substitution is sterically blocked. Less reaction occurs on the external surface acid sites which are non-selective. The first alkylation step is much more rapid than the second. Furthermore, since ortho-substitution of naphthalene by propylene is sterically prevented, formation of TriPN+ products must involve α -substitution. Consequently, TriPN+ product concentrations also decrease considerably at higher levels of dealumination. Sugi et al. made similar observations on this reaction.⁹ They also showed that the external-surface acid sites of HM128 could be preferentially deactivated to improve β -substitution selectivity, while still maintaining the activity for selective substitution inside the channels. Figure 3 also shows that the ultimate attainable β -substitution selectivity depends on the choice of HM starting material.

The HM catalysts have, on average, 38% of their total pore volume in the mesopore region (20-600 Å diameter). Using XRD line-broadening, we determined the mean crystallite dimensions for HM14, HM74 and HM110 to be $0.23 \pm 0.02 \mu\text{m}$, and for HM230, $0.14 \pm 0.01 \mu\text{m}$.⁵ Laser-scattering measurements reported by the manufacturer show that the mordenite starting materials have average particle sizes of about $10 \mu\text{m}$. It is likely that most of the mesopore volume is in the interstices between crystals in the catalyst particles, and dealumination increases the interstitial (mesopore) volume.

The constraints of the microporous channels not only gives rise to the desired regioselective alkylations, but also impede diffusion of the desired products. If formation of the β -substituted products is diffusion limited, an increase in the mesopore volume should increase the rate of their production. Figure 4 shows that the β -substitution selectivity does, in fact, closely parallel HM mesopore volume. Lee et al. showed a similar trend for isopropylation of biphenyl.¹⁶ To account for concurrent, but less pronounced, increase in micropore volumes, it has been proposed that lattice-bound aluminum is removed from the 4-membered rings that separate the 12-membered rings of the main channels from the neighboring 8-membered ring side-pockets.¹⁸ Lee et al. have suggested that propylene may preferentially diffuse through these 8-membered ring channels that run perpendicular to the main channels, and are inaccessible to naphthalene.¹⁶

Pore volume changes do not seem to explain why the 2,6/2,7 DIPN isomer ratio increases with dealumination, considering these two isomers have nearly identical critical diameters.^{3,6} Horsley et al. used molecular graphics screening and molecular mechanics calculations to provide convincing evidence that 2,6-DIPN, with its slightly more linear structure, has a lower activation energy for diffusion than 2,7-DIPN in the microchannels of HM.⁶ With its isopropyl groups on the same side of the molecule, steric repulsions are maximum when 2,7-DIPN diffuses into the pore windows; whereas, diffusion of 2,6-DIPN is significantly less hindered.⁶ Since the channel diameter is obviously a critical parameter in determining the 2,6/2,7 DIPN ratio, we used X-ray powder diffraction to measure the changes in HM unit cell volumes caused by dealumination. These data are listed in Table 3, where the cited errors limits are the standard errors calculated by the LSQ82 program. Mordenite was the only phase detected in the patterns. HM79 seems to be an anomaly because its cell parameters are much lower than expected. The XRD pattern for this catalyst is of low intensity suggesting that some structural collapse may have occurred during

its dealumination. Still, there is a general trend of unit cell contraction with dealumination, with the largest change being in the *b*-direction. HM71 shows the following magnitudes of contraction relative to HM14: a, 0.59%; b, 0.77%; c, 0.65%; and volume, 2.0%. As shown in Figure 5 for the six samples, excluding the anomalous HM79 data, the 2,6/2,7 DIPN ratio shows an approximate reciprocal relation to the changes in unit cell volume. A probable explanation is that HM dealumination causes a slight shrinkage in the channel diameter that results in more snug fit of the 2,6- and 2,7-DIPN isomers in the channels. Diffusion of 2,7-DIPN becomes even more hindered than in the non-dealuminated HM case.

Isopropylation of Biphenyl. General applicability of the dealumination procedure for improvement of regioselectivity was evaluated by examining biphenyl isopropylation over selected dealuminated mordenites. The experimental results are shown in Table 4 and in Figures 6-7. Greater than 99% of the products are isopropylbiphenyls with a small percentage of other alkylbiphenyls which are not *solely* isopropyl-substituted. Tetra-substitution of biphenyl is not observed. The trends in alkylation regioselectivity are remarkably similar to those observed for the naphthalene reaction. Conversion and DIPB yield increase with initial dealumination, then both decrease at higher $\text{SiO}_2/\text{Al}_2\text{O}_3$ ratios. Formation of 3-MIPB is not effected much by dealumination; whereas, the concentration of 2-MIPB in the product goes to near zero. Neglecting isomers with isopropyl groups ortho to each other, there are 10 possible DIPB isomers. We observe 9 peaks in the GC-MS having *m/z* of 238. At present, only the three DIPB isomers listed in Table 4 can be identified with certainty. Of the remaining 7 isomers, there is the 3,5-isomer, and 6 isomers involving substitution at the 2-position(s). Consequently, it is not so surprising that the concentrations of compounds labeled *other-DIPB* closely parallel the 2-MIPB concentrations.

Overall, isopropylation of biphenyl is a more efficient process than isopropylation of naphthalene. Separation of mono-, di- and polysubstituted products from each other is easy in comparison to separation of positional isomers. Dealuminated HM can give 4,4'-DIPB isomer selectivity over 80%, and an isomer ratio with the next most concentrated isomer, 3,4'-DIPB, of about 8. On the other hand, selectivity for the target 2,6-DIPN isomer is only about 60% with a 2,6/2,7 DIPN not exceeding 2.3 in this work. It should be noted that 2,6-DIPN isomer selectivity of over 65%, with 2,6/2,7 DIPN exceeding 2.6, can be achieved by adding a small amount of water to the reactor or by increasing the reaction temperature,⁵ or by using isopropanol as the alkylating agent.³

Conclusions

Dealumination of HM14 increases the 2,6-DIPN isomer selectivity from 30 to 60%. While a similar trend is observed for dealumination of HM38, lower regioselectivity is obtained. However, HM38 retains reasonable activity to higher $\text{SiO}_2/\text{Al}_2\text{O}_3$ ratios than HM14 does. Both factors demonstrate that performance of the dealuminated catalysts is dependent upon the choice of starting material. In comparison biphenyl isopropylation experiments, it was found that 4,4'-DIPB regioselectivity can be increased from 66 to 87% by HM dealumination. Therefore, increased selectivity for the slimmest diisopropyl-isomer with dealumination is a general property: it occurs with different mordenite starting materials and different, but similar in size and shape, reactant molecules.

Comparing regioselectivity and sorption data, we found that a higher percentage of reaction occurs in the confines of the mordenite channels when the density of non-selective external surface acid sites is diminished by dealumination. Relative diffusion rates seem to be a major controlling factor in determining selectivity. Reducing diffusion resistance by increasing the mesoporous volume in the catalyst particle interstices results in an increase in DIPN yield and 2,6-DIPN isomer selectivity.

As reported elsewhere, 2,6-DIPN has a slightly smaller critical diameter and lower activation energy for diffusion in HM than 2,7-DIPN.^{3,6} We used a careful analysis of the unit cell parameters to show that the 2,6/2,7 DIPN ratio increases as the unit cell volumes decrease with aluminum removal. A probable explanation is that HM dealumination causes a slight shrinkage of the channel diameter, increasing the difference in diffusion rates for 2,6- and 2,7-DIPN.

Acknowledgements

We would like to acknowledge the encouragement and support of Prof. Harold Schobert at the Pennsylvania State University. We would also like to thank the PQ Corporation, Inc. for graciously providing the mordenite starting materials with detailed analytical data, and Prof. Deane K. Smith at the Pennsylvania State University for his assistance in the XRD work.

References

1. Song, C.; Schobert, H. H. Specialty Chemicals and Advanced Materials from Coals: Research Needs and Opportunities *Am. Chem. Soc. Div. Fuel Chem. Prepr.* **1992**, *37(2)*, 524-532.
2. Song, C.; Schobert, H. H. Opportunities for Developing Specialty Chemicals and Advanced Materials from Coals *Fuel Process. Technol.* **1993**, *34*, 157-196.
3. Song, C.; Kirby, S. Shape-Selective Alkylation of Naphthalene with Isopropanol Over Mordenite Catalysts *Microporous Materials* **1994**, *2*, 467-476.
4. Song, C.; Schobert, H. H. Non-Fuel Uses of Coals and Synthesis of Chemicals and Materials *Am. Chem. Soc. Div. Fuel Chem. Prepr.* **1995**, *40(2)*, 249-259.
5. Schmitz, A. D.; Song, C. Shape-Selective Isopropylation of Naphthalene Over Dealuminated Mordenites *Am. Chem. Soc. Div. Fuel Chem. Prepr.* **1994**, *39(4)*, 986-991.

6. Horsley, J. A.; Fellmann, J. D.; Derouane, E. G.; Freeman, C. M. Computer-Assisted Screening of Zeolite Catalysts for the Selective Isopropylation of Naphthalene *J. Catal.* **1994**, *147*, 231-240.
7. Loktev, A. S.; Chekriy, P. S. Alkylation of Binuclear Aromatics with Zeolite Catalysts in "Zeolites and Related Microporous Materials: State of the Art 1994," *Stud. Surf. Sci. Catal.* **1994**, *84*, 1845-1851.
8. Chu, S.-J.; Chen, Y.-W. Isopropylation of Naphthalene Over β Zeolite *Ind. Eng. Chem. Res.* **1994**, *33*, 3112-3117.
9. Sugi, Y.; Kim, J.-H.; Matsuzaki, T.; Hanaoka, T.; Kubota, Y.; Tu, X.; Matsumoto, M. The Isopropylation of Naphthalene Over Cerium-Modified H-Mordenite in "Zeolites and Related Microporous Materials: State of the Art 1994," *Stud. Surf. Sci. Catal.* **1994**, *84*, 1837-1844.
10. Sugi, Y.; Matsuzaki, T.; Hanaoka, T.; Kubota, Y.; Kim, J.-H. Shape-Selective Alkylation of Biphenyl Over Mordenites: Effects of Dealumination on Shape-Selectivity and Coke Deposition *Catal. Lett.* **1994**, *26*, 181-187.
11. Sugi, Y.; Toba, M. Shape-Selective Alkylation of Polynuclear Aromatics *Catalysis Today* **1994**, *19*, 187-212.
12. Tu, X.; Matsumoto, M.; Matsuzaki, T.; Hanaoka, T.; Kubota, Y.; Kim, J.-H.; Sugi, Y. *Catal. Lett.* **1993**, *21*, 71-75.
13. Moreau, P.; Finiels, A.; Geneste, P.; Solofo, J. Selective Isopropylation of Naphthalene Over Zeolites *J. Catal.* **1992**, 487-492.
14. Katayama, A.; Toba, M.; Takeuchi, G.; Mizukami, F.; Niwa, S.-i.; Mitamura, S. Shape-Selective Synthesis of 2,6-Diisopropylnaphthalene Over H-Mordenite Catalyst *J. Chem. Soc., Chem. Commun.* **1991**, 39-40.
15. Fellmann, J. D.; Saxton, J.; Wentzcek, P. R.; Derouane, E. G.; Massioni, P. Process for Selective Diisopropylation of Naphthyl Compounds Using Shape Selective Acidic Crystalline Molecular Sieve Catalysts U. S. Patent No. 5,026,942, 1991.
16. Lee, G. S.; Maj, J. J.; Rocke, S. C.; Garcés, J. M. *Catal. Lett.* **1989**, *2*, 243-248.
17. Hubbard, C. R.; Lederman, S. M.; Pyrros, N. P., "A Least Squares Unit Cell Refinement Program;" National Bureau of Standards: Washington, D.C., and JCPDS—International Centre for Diffraction Data: Swarthmore, PA, July 1983.
18. Mishin, I. V.; Bremer, H.; Wendlandt, K.-P. Synthesis and Properties of High-Silica Zeolites with Mordenite Structure in "Catalysis on Zeolites," (Kalló, D.; Minachev, Kh. M., Eds.); H. Stillman Publishers, Inc.: Boca Raton, FL, 1988, pp 231-275.
19. Seddon, D. The Conversion of Aromatics Over Dealuminised Mordenites *Appl. Catal.* **1983**, *7*, 327-336.

Table 1. Sorption Data and Residual Sodium Content for Mordenite Catalysts

catalyst	Na ₂ O, wt%	surface area, m ² /g			pore volume, cm ³ /g		
		total	micro	meso	total	micro	meso
NaM14 ^a	6.24	466	457	10	0.312	0.174	0.138
HM21 ^b	0.02	606	536	70	0.317	0.207	0.110
HM38 ^c	0.07	512	429	82	0.293	0.167	0.126
HM14	0.19	na ^{b,c}	na	na	na	na	na
HM54	0.15	na	na	na	na	na	na
HM62	<0.01	504	413	91	0.250	0.163	0.087
HM70	<0.01	556	395	161	0.280	0.180	0.099
HM71	<0.01	572	497	75	0.349	0.191	0.125
HM74	<0.01	583	509	74	0.385	0.196	0.148
HM79	0.14	na	na	na	na	na	na
HM90	<0.01	540	471	69	0.313	0.188	0.125
HM93 ^d	0.01	na	na	na	na	na	na
HM110	<0.01	539	480	59	0.362	0.184	0.138
HM140 ^d	0.02	na	na	na	na	na	na
HM230	<0.01	498	437	60	0.342	0.168	0.136

^a Data as reported by supplier. ^b Not available. ^c HM14 and NaM14 are assumed to have very similar sorption properties. ^d Produced by dealumination of HM38.

Table 2. Isopropylation of Naphthalene Test Data for HM14- and HM38-Derived Dealuminated Mordenites

catalyst	conv., %	product distribution, mol%			isomer distribution, mol%			
		MIPN	DIPN	TriPN ^a	2-MIPN ^b	2,6-DIPN ^c	2,7-DIPN ^c	2,6/2,7
HM14	76	63	32	3.6	60	33	19	1.76
HM54	43	75	22	1.2	68	50	24	2.11
HM62	78	61	34	3.9	54	29	16	1.78
HM70	82	52	40	5.6	58	44	20	2.17
HM71	74	59	37	2.3	64	51	22	2.29
HM74	47	75	23	0.6	71	55	25	2.24
HM79	69	65	29	3.6	59	39	21	1.86
HM90	36	79	19	0.9	70	53	24	2.21
HM110	15	84	14	0.4	83	61	30	2.05
HM230 ^d	41	72	25	1.1	74	58	25	2.32
HM38	73	60	34	4.4	58	39	19	1.99
HM93	84	48	43	6.5	62	48	22	2.21
HM140	38	77	21	0.4	73	56	25	2.20

^a Tri- and tetraisopropylnaphthalenes. ^b Mole percent in MIPN products. ^c Mole percent in DIPN products. ^d Calcined at 700 °C.

Table 3. Unit Cell Parameters for HM14-Derived Dealuminated Mordenites Determined from XRD Data Using the JCPDS-NBS*LSQ82 Cell Refinement Program

unit cell parameter	HM14	HM54	HM71	HM74	HM79	HM110	HM230
<i>a</i> , Å	18.163 ± 0.005	18.051 ± 0.004	18.056 ± 0.006	18.091 ± 0.009	17.947 ± 0.016	18.075 ± 0.006	18.047 ± 0.008
<i>b</i> , Å	20.314 ± 0.004	20.162 ± 0.005	20.157 ± 0.007	20.217 ± 0.009	19.866 ± 0.012	20.233 ± 0.006	20.197 ± 0.009
<i>c</i> , Å	7.490 ± 0.002	7.447 ± 0.003	7.441 ± 0.003	7.460 ± 0.003	7.383 ± 0.004	7.463 ± 0.002	7.452 ± 0.003
volume, Å ³	2764 ± 1	2710 ± 1	2708 ± 1	2730 ± 1	2632 ± 2	2730 ± 1	2717 ± 2

Table 4. Isopropylation of Biphenyl Test Data for Selected Dealuminated H-Mordenites

catalyst	conv., %	product distribution, mol%			MIPB isomer distribution, mol%			DIPB isomer distribution, mol%			
		MIPB	DIPB	TriPB	2-	3-	4-	3,3'-	3,4'-	4,4'-	other
HM14	49	74	25	0.5	9.2	24	66	3.9	17	66	13.8
HM21	60	64	33	1.5	8.1	26	66	3.0	15	72	10.8
HM38	71	54	42	3.0	10.2	28	62	2.7	13	72	12.2
HM71	46	62	37	1.1	3.1	24	73	1.3	11	83	4.9
HM230	23	67	32	0.5	2.0	18	80	0.9	10	87	2.5

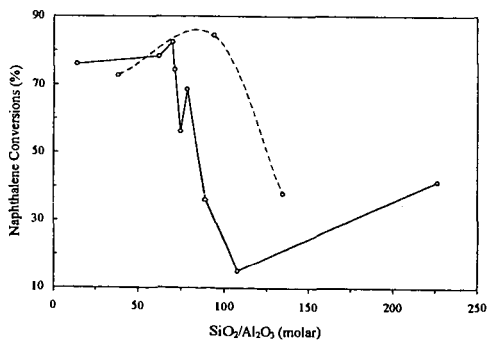


Figure 1. Naphthalene conversions for HM14-derived (solid line) and HM38-derived (broken line) catalysts as a function of SiO₂/Al₂O₃ ratio.

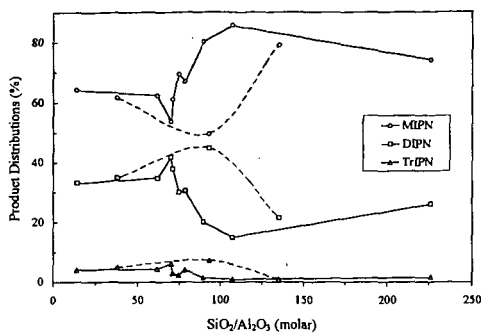


Figure 2. Naphthalene isopropylation product distributions for HM14-derived (solid lines) and HM38-derived (broken lines) catalysts as a function of $\text{SiO}_2/\text{Al}_2\text{O}_3$ ratio.

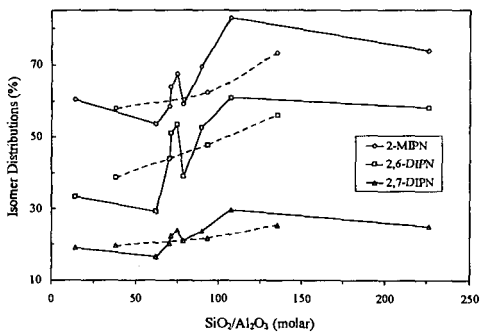


Figure 3. Naphthalene isopropylation isomer distributions for HM14-derived (solid lines) and HM38-derived (broken lines) catalysts as a function of $\text{SiO}_2/\text{Al}_2\text{O}_3$ ratio.

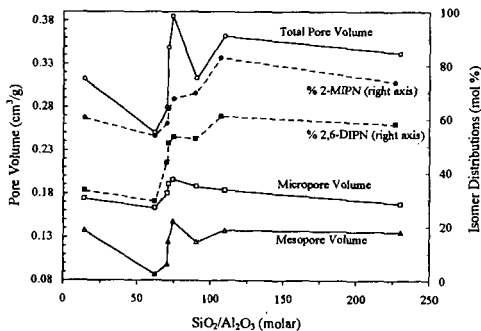


Figure 4. Comparison of pore volumes (solid lines) and β -substitution selectivities (broken lines) for dealuminated HM14 catalysts as a function of $\text{SiO}_2/\text{Al}_2\text{O}_3$ ratio.

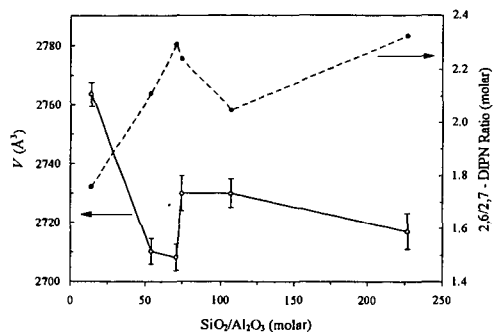


Figure 5. Comparison of unit cell volumes (solid line, left axis) with 2,6/2,7 DIPN ratios (broken line, right axis) for dealuminated HM14 catalysts as a function of $\text{SiO}_2/\text{Al}_2\text{O}_3$ ratio. Error bars represent four-times the standard error in unit cell volumes from Table 3.

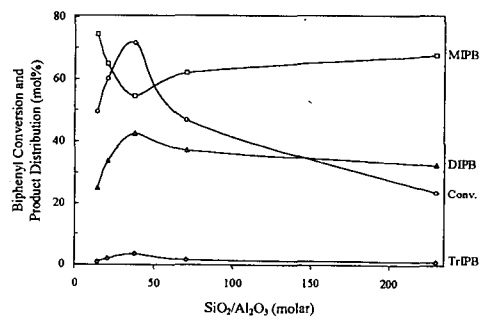


Figure 6. Isopropylation of biphenyl conversion and product distribution as a function of $\text{SiO}_2/\text{Al}_2\text{O}_3$ ratio.

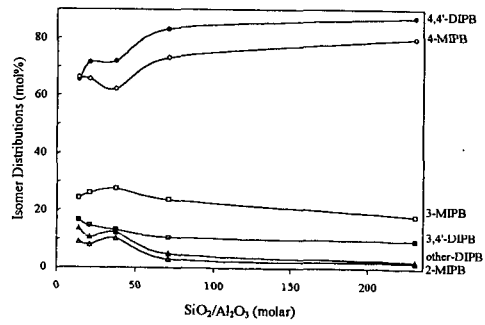


Figure 7. Biphenyl isopropylation isomer distributions as a function of $\text{SiO}_2/\text{Al}_2\text{O}_3$ ratio.